Synthesis and Characterization of Amphiphilic Lipopolymers for Micellar Drug Delivery

Feng Li, Michael Danquah, and Ram I. Mahato*

Department of Pharmaceutical Sciences, University of Tennessee Health Science Center, Memphis, Tennessee 38103

Received May 24, 2010; Revised Manuscript Received July 23, 2010

The objective of this study was to design lipopolymers for hydrophobic drug delivery. Poly(ethylene glycol)-*block*-poly(2-methyl-2-carboxyl-propylene carbonate-graft-dodecanol) (PEG-PCD) lipopolymers were synthesized and characterized by ^{1}H NMR, FT-IR, GPC, and DSC. The critical micelle concentration (CMC) of PEG-PCD micelles was around 10^{-8} M and decreased with increasing length of hydrophobic block. PEG-PCD micelles could efficiently load a model drug embelin into its hydrophobic core and significantly improve its solubility. The loading capacity was dependent on the polymer core structure, but the length of hydrophobic core had little effect. PEG-PCD formed both spherical and cylindrical micelles, which were dependent on the copolymer structure and composition. PEG-PCD lipopolymers with various hydrophobic core lengths showed similar drug release profiles, which were slower than that of poly(ethylene glycol)-*block*-poly(2-methyl-2-benzoxycarbonyl-propylene carbonate) (PEG-PBC) micelles. Embelin loaded PEG-PCD micelles showed significant inhibition of C4-2 prostate cancer cell proliferation, while no obvious cellular toxicity was observed for blank micelles.

1. Introduction

Many anticancer agents are poorly soluble in water, which can cause serious problems for their clinical application. Dimethyl sulfoxide (DMSO), Ctenophore EL, Tween 80, or other surfactants are commonly used to solubilize these drugs. However, these solubilizing agents are harmful to the liver and kidney and cause dose-dependent hemolysis and acute hypersensitivity reactions.[1,2] In addition, because of high critical micelle concentration (CMC) values associated with low molecular weight surfactant micelles, they are not stable after systemic administration and thus result in the precipitation of solubilized drugs.

Poly(ethylene glycol)(PEG)-lipid conjugates, such as PEG-phosphatidylethanolamie (PEG-PE) have been used for micellar drug delivery.[3,4] The use of PEG-lipid conjugates for drug delivery are superior to conventional small molecular weight surfactants, because PEG-lipid conjugates have lower critical micelle concentration (CMC: $\sim 10^{-5}$ M) than conventional surfactants (CMC: $\sim 10^{-3}$ M), suggesting PEG-lipid conjugate micelles are more stable than those formed by conventional surfactants. A typical PEG-lipid conjugate structure includes a hydrophilic PEG corona and a hydrophobic lipid core, which, in turn, is composed of two lipid chains varying from C12 to C18 in chain length. Although we could conjugate PEG with different lipids to make different PEG-lipid conjugates, the flexibility in the design of hydrophobic core is still limited.

Alternatively, amphiphilic copolymers have become promising materials for micellar drug delivery. Pluronic is a triblock copolymer composed of a central hydrophobic chain of poly(propylene oxide) (PPO) flanked by two hydrophilic chains of poly(ethylene glycol) (PEG) and has been widely used for drug delivery.[5] It not only increases drug solubility, but also overcomes drug resistance in cancer.[6,7] The CMC of Pluronic copolymers ranges from 5.3×10^{-3} to 2.8×10^{-6} M, depending on the molecular weight and composition of copolymers.[5] However, the use of Pluronic for drug delivery is somewhat problematic because they are nonbiodegradable. Therefore, biodegradable copolymers such as PEG-PLLA-PEG were designed to facilitate the elimination of polymers from the body.[8] In addition, the structure and size of hydrophobic core block could be properly designed to improve the micelle stability and drug loading. A significantly reduced CMC (10^{-6} to 10^{-7} M) is observed in a diblock copolymer, which is 10 to 100 folds lower than PEG-lipid conjugates.[9] For examples, the CMC of PEG_{5100}-PLA_{4500} was around 3×10^{-6} M, as determined by Danquah et al.[10] Similar results were also reported by Yasugi et al.,[11] who showed that the CMC of PEG_{5700}-PLA_{5400} was around 3×10^{-7} M. The low CMC of micelles formed by amphiphilic copolymers indicates that they are more stable than PEG-lipid conjugate micelles and can maintain the integrity of micelles upon dilution. In addition, we and others have showed that the drug solubility has been significantly improved by properly designing the hydrophobic core structure to improve the compatibility between the hydrophobic core and drugs.[12] For an example, PEG-*b*-poly(*N*-alkyl stearate L-aspartamide), a lipid conjugated polymer, has been used to improve the solubility of a hydrophobic drug, amphotericin B, and demonstrated the possibility of using lipopolymers for solubilization of lipidlike drugs.[13–14]

In this study, we synthesized a novel amphiphilic lipopolymer, poly(ethylene glycol)-*block*-poly(2-methyl-2-carboxyl-propylene carbonate-graft-dodecanol) (PEG-PCD). The polymer synthesis procedures were optimized and the properties of polymers were characterized. PEG-PCD lipopolymers could form micelles and effectively incorporate embelin and improve its water solubility. PEG-PCD lipopolymers were compared with similar polymers with different core structures to investigate the effect of core structure on micelle properties, such as stability, drug loading, particle size and morphology, and in vitro drug release. In addition, we also investigated the effect of hydrophobic core size on the properties of PEG-PCD lipopolymer micelles.

* To whom correspondence should be addressed. Tel.: 901-448-6929. Fax: 901-448-2099. E-mail: rmahato@uthsc.edu.
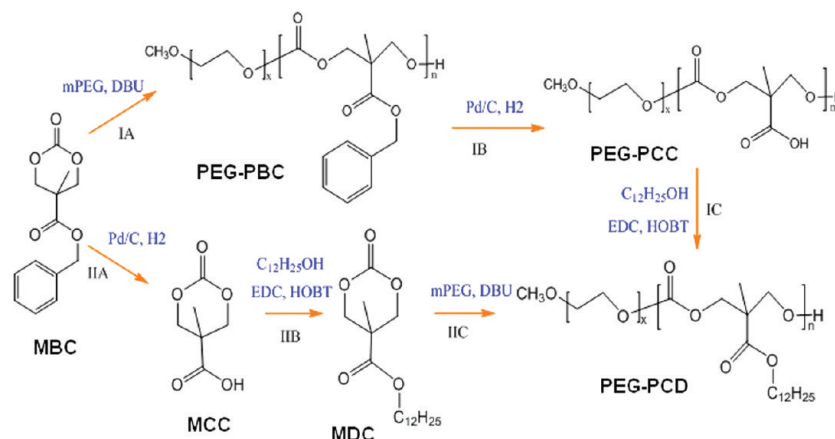
Figure 1. Synthesis of PEG-PCD lipopolymer. Conditions: (**IA**) DBU, CH$_2$Cl$_2$, RT, 3 h. (**IB**) Pd/C (10%), H$_2$, THF/methanol (1:1), RT, 18 h. (**IC**) EDC, HOBT, TEA, DMF, RT, 18 h. (**IIA**) Pd/C (10%), H$_2$, EtOAc, RT, 3 h. (**IIB**) EDC, HOBT, TEA, DMF, RT, 18 h. (**IIC**) DBU, CH$_2$Cl$_2$, RT, 3 h.

Finally, the anticancer activities of embelin loaded micelles were determined in vitro with prostate cancer cells.

2. Experimental Section

2.1. Materials. Hydroxybenzotriazole (HOBT), 1-ethyl-3-(3-dimethylaminopropyl)carbodiimide (EDC), dodecanol, triethylamine (TEA), stannous 2-ethylhexanoate (Sn(Oct)$_2$), diethyl zinc (Et$_2$Zn), 1,8-diazabicyclo[5.4.0]undec-7-ene (DBU), 2,2-bis(hydroxymethyl) propionic acid, methoxy poly(ethylene glycol) (mPEG, M_n = 5000, PDI = 1.03), and all other reagents were purchased from Sigma Aldrich (St. Louis, MO) and used as received.

2.2. Synthesis of Poly(ethylene glycol)-*block*-poly(2-methyl-2-carboxyl-propylene carbonate-graft-dodecanol) (PEG-PCD). PEG-PCD lipopolymer was synthesized using the following two methods (Figure 1):

Method I. (A) Synthesis of Poly(ethylene glycol)-block-poly(2-methyl-2-benzoxycarbonyl-propylene carbonate) (PEG-PBC). Monomer 2-methyl-2-benzyloxycarbonyl-propylene carbonate (MBC) was synthesized as described by Danquah et al.[12] Briefly, a mixture of 0.168 mol 2,2-bis(hydroxymethyl)propionic acid and 0.169 mol potassium hydroxide was dissolved in 125 mL of dimethylformamide (DMF) by heating to 100 °C for 1 h with stirring. Then, 0.202 mol benzyl bromide was added dropwise to the warm solution and stirred at 100 °C for 16 h. At the end of reaction, the solvent was removed under reduced pressure. The residue was dissolved in 150 mL of ethyl acetate, washed with water, and dried over MgSO$_4$. The solvent was removed to yield a crude product, which was recrystallized from toluene to give pure benzyl 2,2-bis(methylol)propionate. Then, 0.05 mol benzyl 2,2-bis(methylol)-propionate was dissolved in 150 mL of CH$_2$Cl$_2$ containing 25 mL of pyridine, and the solution was chilled to 78 °C. A solution of CH$_2$Cl$_2$ containing 25 mmol triphosgene was dripped into the solution over 1 h. The reaction mixture was stirred for an additional 2 h at the room temperature before quenched with 75 mL of saturated aqueous NH$_4$Cl. Subsequently, the organic layer was sequentially washed with aqueous HCl (1 M, 300 mL) and saturated aqueous NaHCO$_3$ (300 mL), dried with Na$_2$SO$_4$, and evaporated to give 2-methyl-2-benzyloxycarbonyl-propylene carbonate (MBC) as a crude product, which was further recrystallized from ethyl acetate to give white crystals.

Three methods with different catalysts were investigated in this study to synthesize PEG-PBC from copolymerization of mPEG with monomer MBC. (1) Sn(Oct)$_2$ (10 mol % relative to mPEG) was added to the mixture of given amounts of mPEG and MBC dissolved in anhydrous toluene in a dried polymerization flask under the protection of a nitrogen atmosphere. To optimize the reaction condition, the reaction mixture was heated to 80 °C for 3 and 16 h under stirring, respectively. (2) DBU (40 μL) was added to the mixture of a given amount of mPEG

and MBC dissolved in 10 mL of anhydrous CH$_2$Cl$_2$ and reacted at RT for 3 h under stirring. (3) Et$_2$Zn (10 mol % relative to mPEG) was added to the mixture of given amount of mPEG and MBC dissolved in anhydrous toluene in a dried polymerization flask under the protection of nitrogen atmosphere and reacted at 80 °C for 16 h under stirring. At the end of reaction, the reaction mixture was dissolved in CHCl$_3$ and the product was precipitated with a large amount of ice-cold diethyl ether and dried under vacuum at room temperature.

(B) Hydrogenation of PEG-PBC. To remove protective benzyl groups, PEG-PBC was subjected to hydrogenation. Briefly, 1 g of PEG-PBC was dissolved in 12 mL of tetrahydrofuran (THF) and methanol mixture (1:1) containing 200 mg palladium on charcoal (Pd/C). The reaction flask was purged with N$_2$ thrice and charged with H$_2$ using a balloon. The reaction was carried out for 18 h with stirring. At the end of reaction, Pd/C was removed by centrifugation. The solvent was removed under reduced pressure to get poly(ethylene glycol)-*block*-poly(2-methyl-2-carboxyl-propylene carbonate) (PEG-PCC).

(C) Lipid Conjugation to PEG-PCC. For lipid conjugation to PEG-PCC, 300 mg PEG-PCC, 260 mg dodecanol, 223 mg hydroxybenzotriazole (HOBT), and 317 mg 1-ethyl-3-(3-dimethylaminopropyl) carbodiimide (EDC) were dissolved in 10 mL of DMF and 340 μL of triethylamine (TEA) was then added to the mixture with stirring. After reaction for 18 h, products were precipitated with a large amount of cold isopropyl alcohol twice and diethyl ether once and then dried under vacuum at room temperature to afford poly(ethylene glycol)-*block*-poly(2-methyl-2-carboxyl-propylene carbonate-*graft*-dodecanol) (PEG-PCD).

Method II. (A) Synthesis of 2-Methyl-2-carboxyl-propylene Carbonate (MCC). MCC was synthesized by hydrogenation of MBC, as described previously.[12] Briefly, 1 g of monomer MBC was dissolved in 10 mL of ethyl acetate containing 100 mg Pd/C. The reaction flask was purged with N$_2$ three times and charged with H$_2$ to 45 psi. The reaction was carried out for 3 h. Then, Pd/C was removed by centrifugation. The solvent was removed under reduced pressure to give MTC-OH as a white crystal.

(B) Synthesis of 2-Methyl-2-dodecanoxycarbonyl-propylene Carbonate (MDC). To synthesize MDC, 480 mg MTC-OH, 465 mg dodecanol, 506 mg HOBT, and 720 mg EDC were dissolved in 20 mL of DMF and 490 μL of TEA was then added to the mixture with stirring for 18 h. The reaction mixture was diluted with ethyl acetate (20 mL), washed with water, and dried over MgSO$_4$. The solvent was removed under reduced pressure to yield a crude product, which was further purified by column chromatography to get MDC as a white powder.

(C) Synthesis of PEG-PCD from Copolymerization of mPEG with MDC. DBU (40 μL) was added to the mixture of a given amount of mPEG, and MDC was dissolved in anhydrous CH$_2$Cl$_2$ and reacted under stirring for 3 h. The reaction mixture was dissolved in CHCl$_3$, and the

product was precipitated with a large amount of cold isopropyl alcohol and diethyl ether and dried under vacuum at room temperature to get PEG-PCD lipopolymer.

2.3. Polymer Characterization. *2.3.1. Nuclear Magnetic Resonance (NMR).* ^{1}H NMR spectra were recorded on a Varian (500 MHz) using deuterated chloroform (CDCl[3]) as a solvent, unless otherwise noted. The chemical shifts were calibrated using tetramethylsilane as an internal reference and given in parts per million.

2.3.2. Infrared (IR) Spectra. The composition of synthesized polymers was also confirmed with infrared (IR) spectra using a Perkin-Elmer IR spectrometer.

2.3.3. Gel Permeation Chromatography (GPC). The weight (M_w) and number (M_n) average molecular weight and polydispersity index (PDI) of synthesized polymers were determined by a Waters GPC system equipped with a GPC column (AM Gel $10^3/5$) and a differential refractive index detector. THF was used as an eluent at a flow rate of 1 mL/min. A series of narrow polystyrene standards (700−40000 g/mol) were used for calibration.

2.3.4. Differential Scanning Calorimetry (DSC). The thermal properties, including glass transition temperature (T_g), melting temperature (T_m), crystalline temperature (T_c) of the synthesized polymers were determined by differential scanning calorimetry (DSC; TA Instrument DSC Q2000 module). Samples were placed in aluminum pans under nitrogen heated from 25 to 100 °C, cooled to −70 °C to remove thermal history, and heated from −70 to 100 °C at a rate of 5 °C/min.

2.4. Critical Micelle Concentration. Critical micelle concentration (CMC) was determined with fluorescent spectroscopy using pyrene as a hydrophobic fluorescent probe, as previously described.[11] Briefly, 40 μL of pyrene stock solution (2.4×10^{-3} M) in acetone was added to 40 mL of water to prepare a saturated pyrene aqueous solution. Polymer samples were dispersed in water with concentration ranges from 0.5 to 4.8×10^{-7} mg/mL and mixed thoroughly with above pyrene solution at a volume ratio of 1:1. The fluorescent intensity was recorded with a Molecular Devices SpectraMax M2/M2e spectrofluorometer (Sunnyvale, CA) with a E_X = 338 nm (I_3) and 333 (I_1) and E_m = 390 nm. The intensity ratio (I_{338}/I_{333}) was plotted against the logarithm of polymer concentration. The CMC value was obtained as the point of intersection of two tangents drawn to the curve at high and low concentrations, respectively.

2.5. Preparation of Polymeric Micelles. Polymeric micelles were prepared with a film dispersion method as previously reported with some modifications.[15] Briefly, 15 mg polymer and a given amount of embelin were dissolved in 0.5 mL of CH[2]Cl[2], and then the solvent was removed under reduced pressure. The resulting film was hydrated in 3 mL of PBS (pH 7.4) and sonicated for 1 min. Then, the residue-free drug was removed by centrifugation at 12000 rpm for 5 min. The supernatant was filtered using a 0.22 μM filter.

2.6. Drug Loading and Encapsulation Efficiency. To determine drug loading, 10 μL of embelin-loaded micelle solution was diluted with methanol. Then drug concentration was determined using a UV spectrometer at 310 nm (Thermo Spectronic). Embelin concentration was calculated based on the UV absorbance using a standard curve. Drug loading and encapsulation efficiency were then determined using the following equations, respectively.

$$\text{drug loading}(\%) = \\ (\text{amount of loaded drug/amount of polymer}) \times 100\%$$

$$\text{drug encapsulation efficiency}(\%) = \\ (\text{amount of loaded drug/amount of drug added}) \times 100\%$$

$$\text{theoretical loading}(\%) = \\ (\text{amount of drug added/amount of polymer}) \times 100\%$$

Theoretical loading is equal to drug loading when the loading efficiency is 100%.

2.7. Morphology and Particle Size. The particle size of polymeric micelles was determined by dynamic light scattering (Malvern Nano ZS). The intensity of scattered light was detected at 90°. The particle size measurement was repeated three times and the data were reported as the mean ± SD. The morphology of polymeric micelles were observed using a transmission electron microscope (TEM, JEM-100S) using an acceleration voltage of 60 kV. Micelles was loaded on a copper grid and stained with 1% uranyl acetate. The grid was visualized under the electron microscope with magnifications of 75,000.

2.8. In Vitro Drug Release. The dialysis technique was employed to determine the release of embelin from polymeric micelles in PBS (pH 7.4) with 0.1% Tween-80. The micelles used for in vitro release study have a polymer concentration of 5 mg/mL. A total of 800 μL of micelles with 5% drug loading were used to compare the release profiles of PEG-PCD with different PCD length. In addition, 2 mL micelles with 2% drug loading were also used to compare the release profiles of PEG[114]-PCD[29] and PEG[114]-PBC[30]. Embelin-loaded micelles were placed into a dialysis tube with a molecular weight cutoff of 3500 Da and dialyzed against 50 mL of release medium in a thermocontrolled shaker with a stirring speed of 180 rpm at 37 °C. At specified time, 1 mL release medium was withdrawn and embelin concentration was determined with a UV spectrophotometer based on UV absorbance at 310 nm. All experiments were performed in triplicate and the data reported as the mean of the three individual experiments. The release profiles were assessed as described previously[16] using a similarity factor (f2). The percentage of cumulative drug release was calculated with the following equation:

$$\text{cumulative drug release}(\%) = \\ \frac{\text{cumulative amount of released drug}}{\text{total amount of drug added}} \times 100\%$$

2.9. In Vitro Cytotoxicity of Embelin-Loaded Micelles. C4-2 prostate cancer cell line was used to determine the cell growth inhibition ability of embelin-loaded micelles. Cells were cultured in RPMI 1640 media supplemented with 10% fetal bovine serum (FBS) and 1% antibiotic-antimycotic at 37 °C in humidified environment of 5% CO[2]. Cells were seeded in 96-well plates at a density of 5000 cells per well 18 h before treatment. Then, cells were treated with drug-loaded micelles or equivalent amount of blank micelles for additional 72 h. At the end of treatment, cell culture medium was replaced by 100 μL of medium with 0.5 mg/mL 3-(4,5-dimethyl-thiazol-2-yl)-2,5-diphenyl tetrazolium bromide (MTT) and incubated for 1 h at 37 °C. Then the medium was carefully removed and 200 μL of DMSO was added into each well to dissolve the formazan crystals. The absorbance was measured in a microplate reader at a wavelength of 560 nm. Cell viability was expressed as the percentage of control group.

$$\text{cell viability}(\%) = A_{\text{test}}/A_{\text{control}} \times 100\%$$

3. Results

3.1. Synthesis and Characterization of Polymers. As summarized in Figure 1, the target lipopolymer PEG-PCD was synthesized by two approaches. In the first approach, PEG was copolymerized with MBC to afford poly(ethylene glycol)-*block*-poly(2-methyl-2-benzoxycarbonyl-propylene carbonate) (PEG-PBC). Then, the pendant benzyl group was removed by hydrogenation to expose carboxyl groups to get poly(ethylene glycol)-*block*-poly(2-methyl-2-carboxyl-propylene carbonate) (PEG-PCC). Finally, poly(ethylene glycol)-*block*-poly(2-methyl-2-carboxyl-propylene carbonate-*graft*-dodecanol) (PEG-PCD) lipopolymer was synthesized by conjugating dodecanol to the carboxyl groups. In the second approach, PEG was copolymerized with a lipid modified monomer 2-methyl-2-dodecanoxy-carbonyl-propylene carbonate (MDC). MCC and MDC were

Table 1. Effect of Different Catalyst on the Polymerization of PEG-PBC Copolymer

catalyst[a]	[MBC]/[PEG-OH][e]	$M_{n,target}$[f]	DP_{MBC}[g]	M_n[h]	conversion (%)[i]
DBU[b]	10	7500	8	7000	80
DBU[b]	20	10000	17	9250	85
DBU[b]	34	13500	30	12500	88
Sn(oct)₂[c]	34	13500	17	9250	50
Sn(oct)₂[d]	34	13500	22	10500	65
Et₂Zn[d]	20	10000	6	6500	30

[a] DBU, 1,8-diazabicyclo[5.4.0]undec-7-ene; Sn(oct)₂, stannous 2-ethylhexanoate; Et₂Zn, diethy zinc. [b] Reaction condition: RT, 3 h. [c] Reaction condition: 80 °C, 3 h. [d] Reaction condition: 80°, 16 h. [e] Molar ratio of monomer (MBC) to PEG in the feed. [f] $M_{n,target}$ = [MBC]/[PEG−OH] × $M_{monomer\ unit}$ (250) + M_{PEG-OH} (5000). [g] DP: degree of polymerization, determined by ^{1}H NMR. [h] M_n = DP × $M_{monomer\ unit}$ (250) + M_{PEG-OH} (5000). [i] Determined by ^{1}H NMR, conversion (%) = DP/([MBC]/[PEG-OH]) × 100%.

characterized with ^{1}H NMR (Figure S1) and ESI-MS. MCC: ^{1}H NMR (500 MHz, DMSO) δ 13.35 (s, 1H), 4.57 (d, 2H), 4.32 (d, 2H), 1.18 (s, 3H). MS (ESI) *m/z* 159 [M-H]⁻. MCC: ^{1}H NMR (500 MHz, CDCl₃) δ 4.50 (d, 2H), 4.2 (d, 4H), 1.65 (m, 2H), 1.4−1.2 (m, 21H), 0.85 (t, 3H). MS (ESI) *m/z* 351 [M + Na]⁺. Although we could synthesize the lipopolymers with both approaches, the second approach involves column purification of MDC, which is a time-consuming process. Therefore, the first approach was selected to generate lipopolymer PEG-PCD.

To achieve the optimal polymerization efficiency, three different catalysts were tested for copolymerization of PEG and MBC, as summarized in Table 1. Among three catalysts tested, DBU was the best, as the conversion rate was 80−88% at the molar ratio of monomer and PEG ranging from 10 to 34. Both Sn(oct)₂ and Et₂Zn were used at 80 °C and the degree of polymerization (DP) was increased with prolonged reaction time from 3 to 16 h for Sn(oct)₂. However, both of these two catalysts gave less DP under the reaction conditions described in Table 1. Therefore, DBU was selected in the current study.

The structures of PEG-PBC, PEG-PCC, and PEG-PCD were confirmed by ^{1}H NMR (Figure 2). From Figure 2A, the following peaks were observed for PEG-PBC polymer at δ 1.2 (CH₃ in BC unit), δ 3.6 (CH₂ in PEG), δ 4.3(CH₂ in BC main chain), δ 5.2 (CH₂ in BC side group), and δ 7.3 (phenyl ring). All signals are assigned as methoxy poly(ethylene glycol) (mPEG) and polymerized BC units. In addition, the success of polymerization was confirmed by the disappearance of signal at δ 4.2 and 4.6 in the MBC monomer and appearance of a new peak at δ 4.3. The degree of polymerization and molecular weight of the polymers was estimated based on the peak areas of PEG CH₂ groups at δ 3.6 and those of CH₂ in BC main chain at δ 4.3.

The benzyl groups were removed via Pd/C catalyzed hydrogenation. The peaks at δ 5.2 (CH₂ in BC side group) and δ 7.3 (phenyl ring) disappeared after hydrogenation (Figure 2B), which indicates the complete removal of pendant benzyl group. In addition, a peak at δ 13 was observed, which belongs to the exposed carboxyl group after removing protective benzyl group. Dodecanol was conjugated onto the polymer backbone using EDC/HOBT chemistry. The success of dodecanol conjugation to PEG-PCC carboxyl group was confirmed by the appearance of new peaks at δ 4.1, 1.6, 1.2−1.4, and 0.9, which could be assigned to different groups in the lipid as shown in Figure 2C.

The FT-IR of PEG-PBC, PEG-PCC, and PEG-PCD also confirmed the success of the reaction (Figure 3). In FT-IR spectra of PEG-PBC, there were peaks at 736 and 696 cm⁻¹,
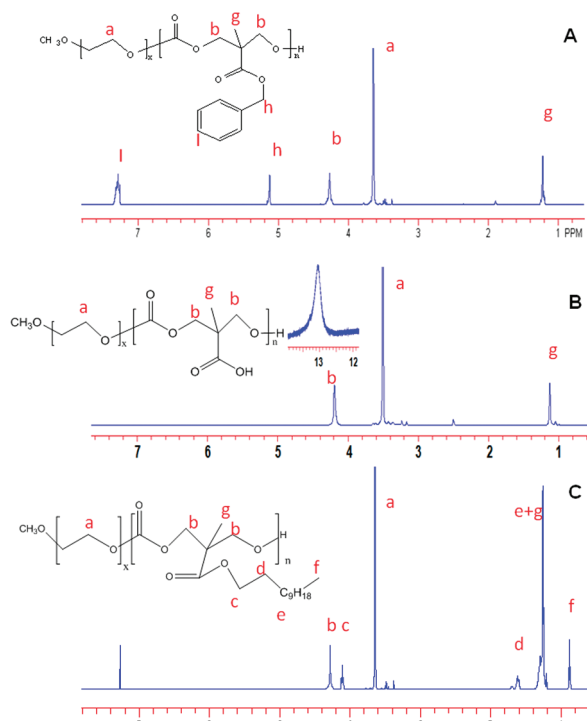
Figure 2. ^{1}H NMR of polymers: (A) PEG₁₁₄-PBC₃₀ in CDCl₃, (B) PEG₁₁₄-PCC₃₀ in DMSO, and (C) PEG₁₁₄-PCD₂₉ in CDCl₃.
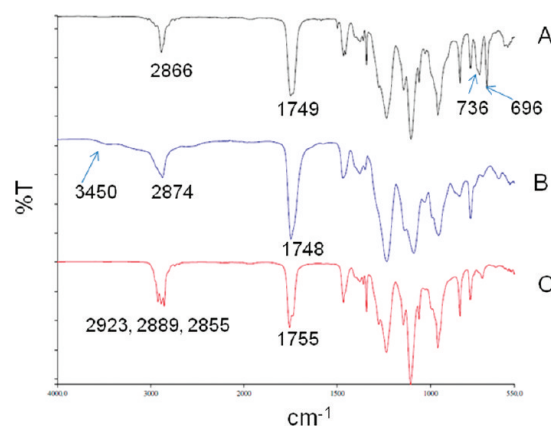
Figure 3. FT-IR spectra of polymers: (A) PEG₁₁₄-PBC₃₀, (B) PEG₁₁₄-PCC₃₀, and (C) PEG₁₁₄-PCD₂₉.

which were due to the CH vibrations of benzyl groups. These two peaks were absent in the FT-IR spectra of PEG-PCC and PEG-PCD, indicating the removal of the pendant benzyl groups during hydrogenation. In addition, we also observed a broad OH stretch band, which was centered at 3450 cm⁻¹ and partially overlapped with C−H stretch. This further confirmed the presence of pendant COOH groups. Besides, we also observed absorbance bands due to the C=O stretching vibration at 1749 cm⁻¹ (PEG-PBC), 1748 cm⁻¹ (PEG-PCC), and 1755 cm⁻¹ (PEG-PCD), respectively. The C−H stretch band was observed at 2886 cm⁻¹ for PEG-PBC, 2874 cm⁻¹ for PEG-PCC. In addition, three bands at 2923, 2889, and 2855 cm⁻¹ were observed for PEG-PCD, indicating the presence of pendant long alkanes.

The characteristics of PEG-PBC, PEG-PCC, and PEG-PCD polymers are summarized in Table 2. The molecular weight of PEG-PBC and PEG-PCC were calculated based on the peak areas of PEG CH₂ groups at δ 3.6 and those of CH₂ in BC main chain at δ 4.3 in the ^{1}H NMR spectrum. In addition, the

Table 2. Characteristics of PEG Copolymers with Different Core Structure

| polymer[a]	M_n (NMR)	M_w (GPC)[b]	M_n (GPC)[b]	PDI[b]	CMC (g/L)	CMC (M)[c]	crystallinity
PEG$_{114}$-PBC$_{30}$	12500	11140	9703	1.15	4.0×10^{-4}	3.2×10^{-8}	semicrystalline
PEG$_{114}$-PCC$_{30}$	9800	7447	6563	1.13	2.2×10^{-2}	2.3×10^{-6}	amorphous
PEG$_{114}$-PCD$_{29}$	13561	13342	11636	1.15	3.6×10^{-4}	2.6×10^{-8}	crystalline
PEG$_{114}$-PCD$_{16}$	10248	11794	9590	1.23	9.0×10^{-4}	$8.7 \times ^{-8}$	crystalline
PEG$_{114}$-PCD$_{6}$	6968	6580	6203	1.06	1.4×10^{-3}	2.0×10^{-7}	crystalline

[a] PEG-PBC, poly(ethylene glycol)-*block*-poly(2-methyl-2-benzoxycarbonyl-propylene carbonate); PEG-PCD, poly(ethylene glycol)-*block*-poly(2-methyl-2-carboxyl-propylene carbonate-graft-dodecanol); PEG-PCC, poly(ethylene glycol)-*block*-poly(2-methyl-2-carboxyl-propylene carbonate). [b] M_w and M_n were apparent molecular weight determined by GPC; PDI = $(M_w/M_n) \times 100\%$. [c] CMC (g/L) normalized with M_n from ^{1}H NMR.
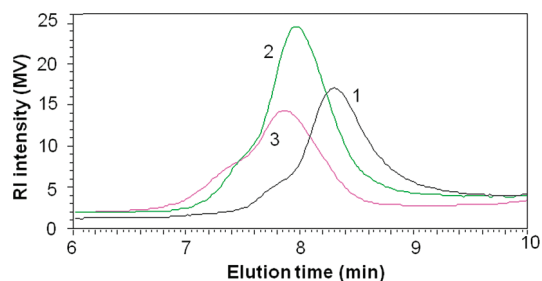
Figure 4. Gel permeation chromatography (GPC) of (1) PEG$_{114}$-PCC$_{30}$ [M_n = 6563 g/mol, M_w/M_n = 1.13]; (2) PEG$_{114}$-PBC$_{30}$ [M_n = 9703 g/mol, M_w/M_n = 1.15]; (3) PEG$_{114}$-PCD$_{29}$ [M_n = 11636 g/mol, M_w/M_n = 1.15].

Figure 5. Thermal analysis of polymers by differential scanning calorimetry (DSC). (A) Polymers of different core structures: PEG$_{114}$-PBC$_{30}$, PEG$_{114}$-PCC$_{30}$, and PEG$_{114}$-PCD$_{29}$. (B) PEG-PCD polymers with different PCD core length: n = 6, 16, and 29.

percentage of conjugation and molecular weight of the lipopolymer was calculated by the peak areas at δ 4.3 (belongs to polymer backbone) and at δ 4.1 (belongs to the conjugated pendant lipid) in the ^{1}H NMR spectrum. The M_n determine by ^{1}H NMR were 12500 g/mol for PEG$_{114}$-PBC$_{30}$, 9800 g/mol for PEG$_{114}$-PCC$_{30}$, 13561 g/mol for PEG$_{114}$-PCD$_{29}$, 10248 g/mol for PEG$_{114}$-PCD$_{16}$, and 6968 g/mol for PEG$_{114}$-PCD$_6$, respectively. GPC was also used to determine the apparent weight (M_w) and number (M_n) average molecular weight of polymers and their polydispersity index. A good correlation was observed between the molecular weight estimated from NMR and M_w or M_n determined by GPC. All of the polymers showed narrow distribution as revealed by the small polydispersity index (1.06−1.23). A representative plot comparing the GPC chromatograms for PEG$_{114}$-PCC$_{30}$, PEG$_{114}$-PBC$_{30}$, and PEG$_{114}$-PCD$_{29}$ was shown in Figure 4.

DSC was used to determine the thermal properties of the synthesized block copolymers. The thermograms of diblock copolymers with different core structures are shown in Figure 5. PEG$_{114}$-PBC$_{30}$ has a T_g = −35.7 °C, T_c = 6.3 °C, and T_m = 49.5 °C, respectively. PEG$_{114}$-PCC$_{30}$, which is a transparent viscous liquid, showed a T_g of −30.7 °C, but no obvious T_c or T_m. PEG$_{114}$-PCD$_{29}$ showed a T_m of −35.7 °C, but no obvious T_g or T_c. The different thermal properties observed with DSC suggesting different properties of the copolymers. Only T_g was observed in PEG$_{114}$-PCC$_{30}$, indicating it is an amorphous polymer. PEG$_{114}$-PCD$_{29}$ has a high degree of crystallinity, because there was no T_g observed. The observed T_g, T_c, and T_m in PEG-PBC indicate the existence of both amorphous domain and crystalline domains in PEG$_{114}$-PBC$_{30}$, which is a semicrystalline polymer. We also calculated the degree of crystallinity based on the DSC peak areas, which was 57.1%. Different degrees of crystallinity of PEG$_{114}$-PCC$_{30}$, PEG$_{114}$-PBC$_{30}$, and PEG$_{114}$-PCD$_{29}$ might be due to the different intermolecular forces among these three polymers with different hydrophobic core structures. We also determined the effect of hydrophobic core size on the T_m of PEG-PCD. As shown in Figure 5B, the T_m for PEG$_{114}$-PCD$_{29}$, PEG$_{114}$-PCD$_{16}$, and PEG$_{114}$-PCD$_6$ were 51.7, 53.6, 55.3 °C, respectively.
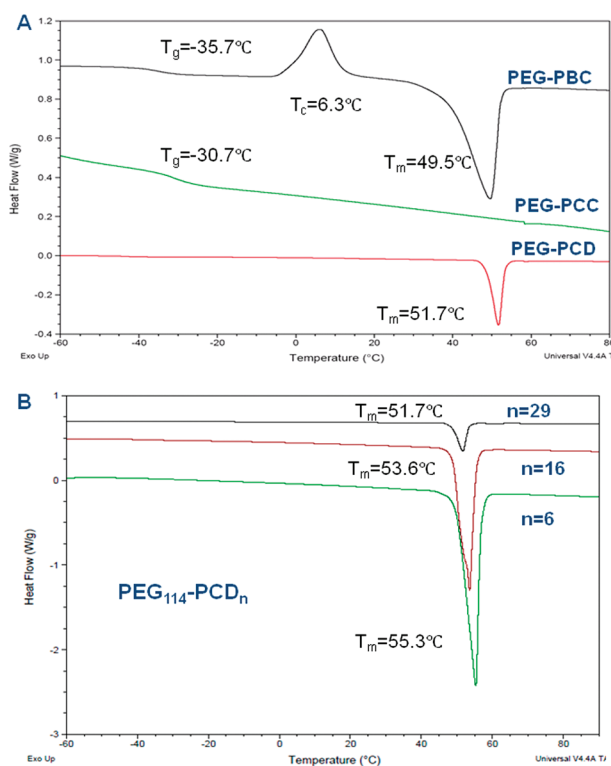
The polymers were further characterized by fluorescence spectroscopy to determine the CMC (Figure 6). PEG$_{114}$-PBC$_{30}$ and PEG$_{114}$-PCD$_{29}$ had low CMC values of 4.0×10^{-4} g/L and 3.6×10^{-4} g/L, respectively. In contrast, the CMC of PEG$_{114}$-PCC$_{30}$ was 2.2×10^{-2} g/L, which was around 50 folds higher than those of PEG$_{114}$-PBC$_{30}$ or PEG$_{114}$-PCD$_{29}$. The low CMC indicates the good stability of micelles prepared from PEG$_{114}$-PBC$_{30}$ and PEG$_{114}$-PCD$_{29}$. The effect of hydrophobic core size on PEG-PCD micelle stability was also determined. The CMC of PEG-PCD micelles decreased significantly from 1.4×10^{-3} g/L to 3.6×10^{-4} g/L when the DP(n) increased from 6 to 29 (Figure 6B).

3.2. Preparation and Characterization of Micelles. *3.2.1. Drug Loading Efficiency.* The amount of embelin loaded into polymeric micelles and loading efficiency were calculated using the equations described in the experimental methods. As demonstrated in Figure 7, PEG-PBC showed 2% drug loading at 5% theoretical loading, which corresponds to 40% loading efficiency, in contrast, 5% drug loading was achieved by PEG-PCD with different hydrophobic core lengths, which corresponds to 100% loading efficiency. Increase in theoretical loading from 5 to 10% showed little effect on the drug loading of PEG-PBC micelles and the loading efficiency decreased correspondingly.
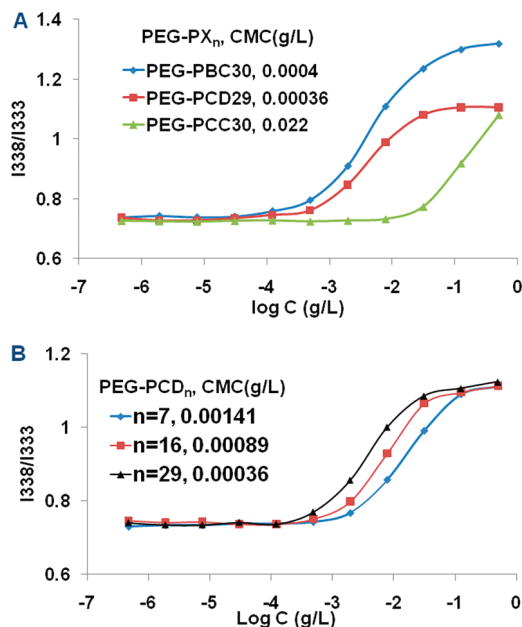
Figure 6. Plots of the intensity ratio I_{338}/I_{333} from pyrene excitation spectra at $\lambda_{em} = 390$ nm vs log C for (A) polymer with different core structures: PEG_{114}-PBC_{30}, PEG_{114}-PCD_{29}, and PEG_{114}-PCC_{30}. (B) PEG-PCD polymers with different PCD core length: $n = 6$, 16, and 29.
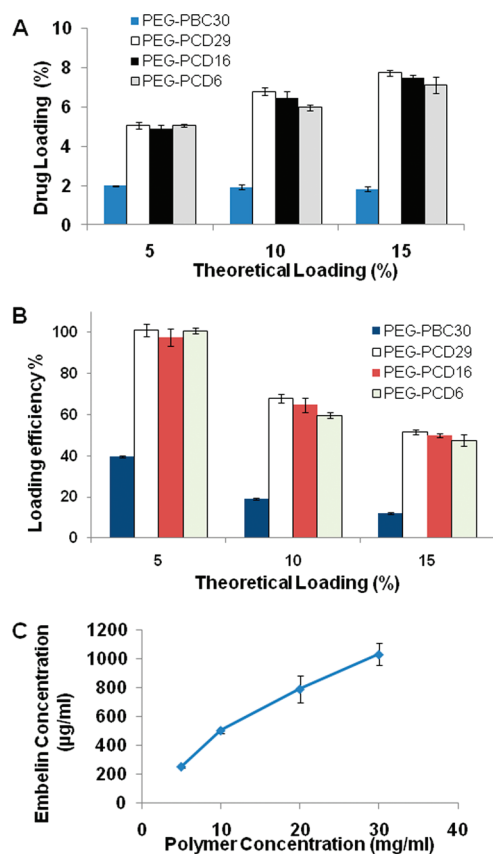
Figure 7. Optimization of embelin-loaded micelle formulations. (A) Effect of hydrophobic core structure and length on drug loading and (B) loading efficiency. Embelin-loaded PEG-PBC and PEG-PCD micelles were prepared at 5, 10, and 15% of theoretical drug loading. (C) Encapsulation of embelin by PEG-PCD micelles as a function of polymer concentration.

However, the drug loading increased from 5 to 6 and 7% for PEG-PCD micelles, when theoretical loading increased from 5
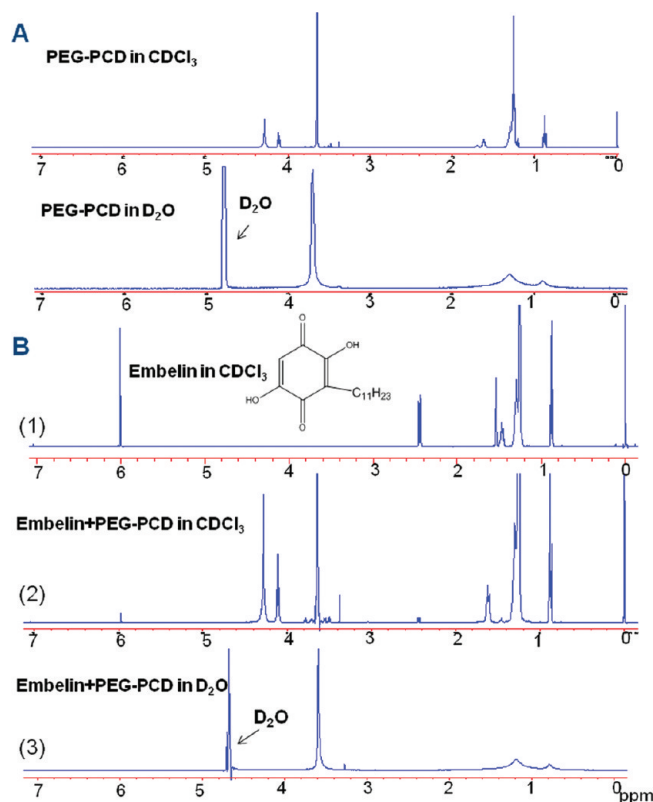

Figure 8. Core–shell structure formed by PEG_{114}-PCD_{29} lipopolymer. (A) ^1H NMR of blank PEG_{114}-PCD_{29} in $CDCl_3$ and D_2O. (B) ^1H NMR of PEG_{114}-PCD_{29} and emblin: (1) free embelin dissolved in $CDCl_3$; (2) embelin and PEG_{114}-PCD_{29} dissolved in $CDCl_3$ at embelin to polymer ratio of 3%; (3) embelin-loaded PEG_{114}-PCD_{29} micelles in D_2O at embelin to polymer ratio of 3%.

to 10 and 15%, with decrease in loading efficiency from 100 to 60 and 50%, respectively. There was no significant difference among three PEG-PCD lipopolymers with different hydrophobic core lengths.

3.2.2. Core–Shell Structure Formation. ^1H NMR spectroscopy was used to demonstrate the formation of core–shell of PEG-PCD lipopolymer micelles (Figure 8). In $CDCl_3$, peaks from both the hydrophilic PEG block (3.6 ppm) and the hydrophobic core block (4.3, 4.1, 1.6, 1.2–1.4, and 0.9 ppm) was observed. In D_2O, all the peaks corresponding to the hydrophobic core block were significantly diminished in contrast to the strong peaks for hydrophilic PEG block (Figure 8A). This is consistent with a core–shell structure with a collapsed hydrophobic core. In addition, we also compared ^1H NMR spectra of embelin-loaded PEG-PCD lipopolymer in $CDCl_3$ and D_2O. Although the specific peaks for embelin at 6 and 2.4 ppm was observed when dissolved in $CDCl_3$, they disappeared when they formed micelles in D_2O. These results indicate that PEG-PCD lipopolymer will form micelles in water with a PEG hydrophilic shell and a hydrophobic core, and embelin is incorporated into the hydrophobic core.

3.2.3. Physical Appearance and Particle Size Distribution. The physical appearance of blank and drug-loaded micelles is shown in Figure 9A. Both PEG-PCD and PEG_{114}-PBC_{30} formed a translucent micelle solution, which was stable at room temperature and showed no precipitation on storage at the room temperature for one week. In contrast, there was a milk-like suspension formation of PEG_{114}-PCC_{30} copolymer micelles and precipitation was observed after overnight storage of these micelles. Also, the drug-loaded micelles showed a pink color
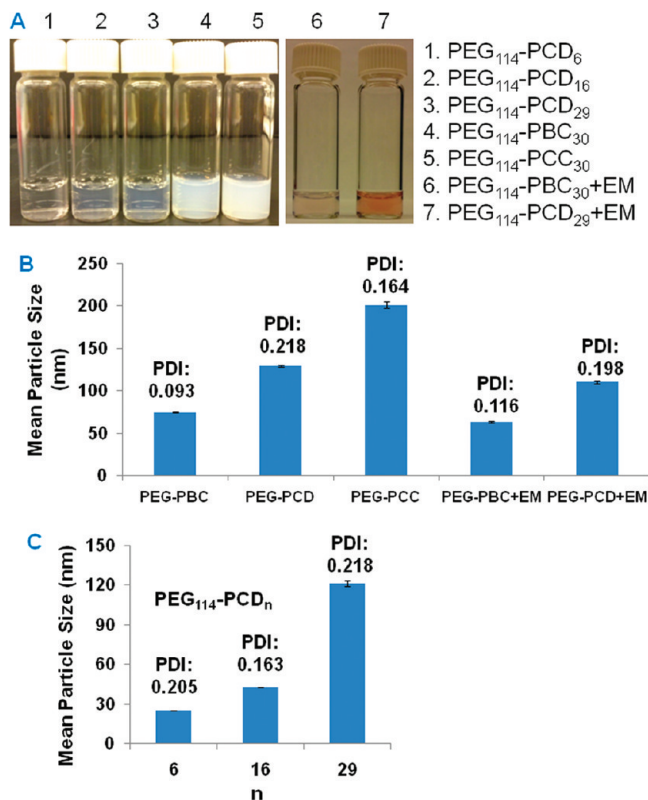
**Figure 9.** Physical appearance and particle size of micelles. (A) Appearance of blank or embelin-loaded micelles prepared from polymers with different core structure and length (polymer concentration 5 mg/mL). (B) Mean particle size of blank or embelin-loaded micelles prepared from PEG_{114}-PCD_{29}, PEG_{114}-PBC_{30}, and PEG_{114}-PCC_{30}. (C) Mean particle size of micelles prepared from PEG-PCD polymers with different PCD core length: $n = 6$, 16, and 29.

due to the solubilized embelin (EM). The color observed in PEG_{114}-PCD_{29} micelles was darker than those of PEG_{114}-PBC_{30} micelles prepared at the same theoretical loading (5%), and this was consistent with the high drug loading in PEG_{114}-PCD_{29} micelles. We also determined the particle size and size distribution of blank and embelin-loaded micelles by dynamic light scattering (Figure 9B). The blank and embelin-loaded PEG_{114}-PCB_{30} micelles had the mean particle size of 74 and 64 nm, respectively. The particle size of blank and embelin-loaded PEG_{114}-PCD_{29} micelles was 129 and 110 nm, respectively. There was no increase in the mean particle size after embelin loading. In contrast, micelles formed by PEG_{114}-PCC_{30} showed a particle size of 204 nm. We also determined the particle size of PEG-PCD with different PCD core lengths; the mean particle sizes were 129 nm for PEG_{114}-PCD_{29}, 42.6 nm for PEG_{114}-PCD_{16}, and 25 nm for PEG_{114}-PCD_6, respectively.

3.2.4. Morphology of Micelles. The morphology of micelles formed by PEG-PBC and PEG-PCD was determined by transmission electron micrography (TEM; Figure 10). PEG-PCD formed micelles with different morphologies and sizes, depending on the ratio of hydrophobic core (Figure 10A−C). PEG_{114}-PBC_{30} formed spherical micelles (Figure 10D). PEG_{114}-PCD_{29} formed both spherical and cylindrical micelles with a diameter less than 50 nm, and the cylindrical micelle was the dominant form. The contour length of the cylindrical micelles ranged from several hundred nanometers to several micrometers. However, PEG_{114}-PCD_{16} and PEG_{114}-PCD_6 formed only spherical micelles. We also determined the morphology of embelin loaded micelles prepared from PEG_{114}-PCD_6, PEG_{114}-PCD_{16}, PEG_{114}-PCD_{29}, and PEG_{114}-PBC_{30}. As shown in Figure S2, the loading of embelin
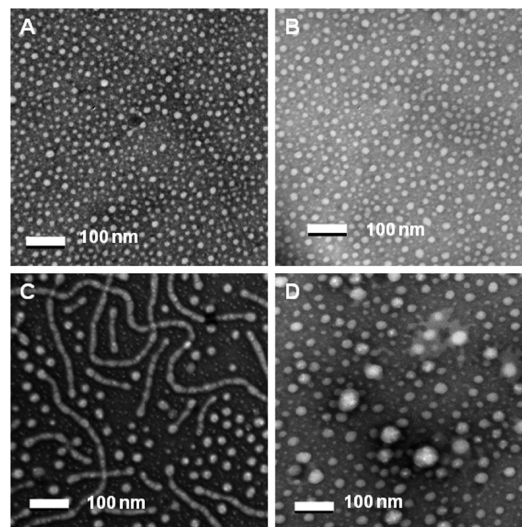
Figure 10. Transmission electron microscopy (TEM) of micelle prepared from (A) PEG_{114}-PCD_6, (B) PEG_{114}-PCD_{16}, (C) PEG_{114}-PCD_{29}, and (D) PEG_{114}-PBC_{30}.
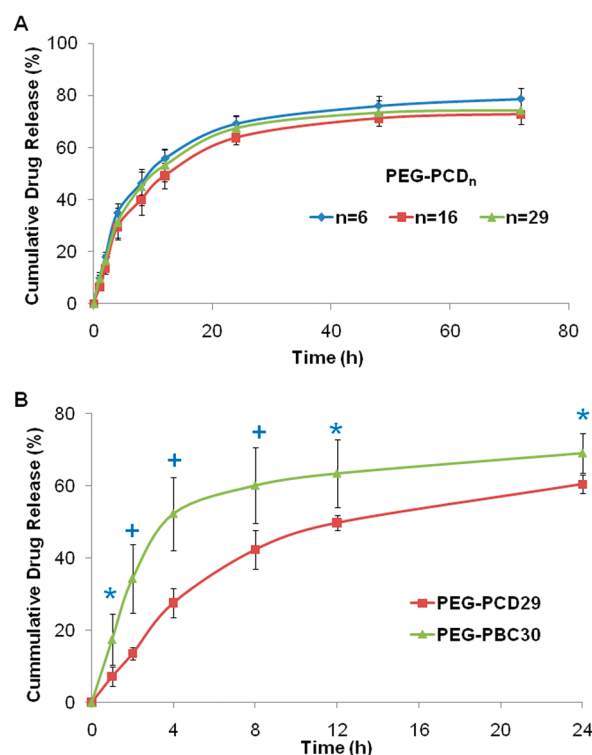
Figure 11. In vitro release of embelin from polymeric micelles. (A) Release profiles of PEG-PCD micelles with different PCD core lengths at drug loading of 5%. (B) Release profiles of PEG_{114}-PCD_{29} and PEG_{114}-PBC_{30} micelles at drug loading of 2%. * $P < 0.05$, + $P < 0.01$, compared with PEG_{114}-PBC_{30} micelles using Student's unpaired t test. Results were expressed as mean ± SD ($n = 3$).

at 5% in PEG-PCD and 2% at PEG_{114}-PBC_{30} had no effect on the morphology of micelles.

3.2.6. In Vitro Drug Release. The cumulative percentage of embelin released from PEG-PCD micelles with different PCD block length was shown in Figure 11A. Similarity factors (f_2) were calculated to compare the drug release profiles of micelles with various hydrophobic core lengths. The similarity factors were 63 ($n = 6$ vs 16), 78 ($n = 6$ vs 29), and 74 ($n = 16$ vs 29), respectively. Therefore, these micelles showed similar release profiles because the release profiles are considered as the same when the similarity factors are greater than 50. The
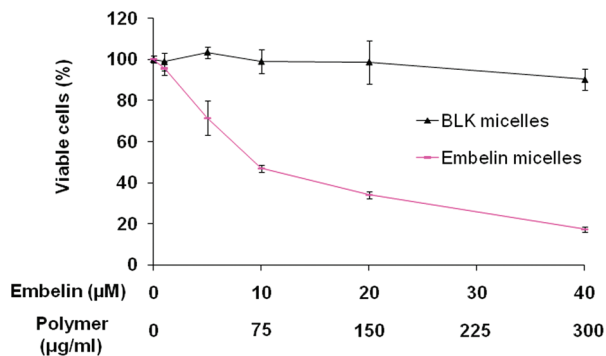
Figure 12. Inhibition of C4-2 cell proliferation by blank and PEG$_{114}$-PCD$_{29}$ micelle formulated embelin. The weight ratio of embelin and polymer was 4% (embelin/polymer). Blank micelles with same polymer concentration were served as control. Cell viability was determined by MTT assay at 72 h post treatment. Results were expressed as mean ± SD ($n = 4$).

release of embelin from PEG-PCD micelles was fit to a first-order process for the first 24 h. The release half-life was around 12 h. The effect of hydrophobic core on embelin release was also investigated (Figure 11B). The release of embelin from PEG$_{114}$-PCD$_{30}$ was significantly slower compared to PEG$_{114}$-PBC$_{30}$ with a similarity factor of 38. In addition, the embelin release half-life from PEG$_{114}$-PBC$_{30}$ micelles was 4 h, which was much shorter than that of PEG$_{114}$-PCD$_{30}$.

3.2.7. Bioevaluation of Drug Loaded Micelles. The anticancer activity of embelin loaded PEG-PCD micelles was determined in C4−2 prostate cancer cells. As shown in Figure 12, while blank PEG$_{114}$-PCD$_{29}$ polymer showed negligible effect on cell proliferation at polymer concentration up to 0.3 mg/mL, embelin-loaded PEG$_{114}$-PCD$_{29}$ micelles showed significant inhibition of C4-2 cell proliferation in a dose-dependent manner, with the IC$_{50}$ of 10 μM. The free drug dissolved in DMSO showed similar anticancer effects to micelle formulated embelin (data not shown). No direct comparison can be made with the results of embelin formulated in micelles and dissolved in DMSO, as DMSO is known to kill tumor cells and may not be suitable for in vivo applications. However, this finding is significant because the application of polymeric micelles could avoid the use of toxic solubilzing agents such as DMSO, Cremophore EL, and Tween 80.

4. Discussion

Polymeric micelles can serve as a vehicle, which self-assemble into a core−shell structure with a hydrophobic core capable of loading hydrophobic drugs.[17,18] The stealth properties associated with hydrophilic PEG corona of micelles prevent their aggregation, restrict plasma protein adsorption, prevent recognition by the reticuloendothelial system (RES), and minimize their rapid elimination from the bloodstream. The small size of micelles ensures their accumulation preferentially in the tumor via EPR effects.[19,20] However, successful micellar drug delivery into tumor requires the micelles remain stable during blood circulation upon systemic administration. The stability of micelles could be enhanced by cross-linking of the shell, core−shell interface, or the core of the micelles.[21−23] However, the application of chemical cross-linked micelles is limited due to the complexity of cross-linking process, possible effects on the structure and properties of loaded drugs, and problems associated with drug release. Alternatively, the stability of micelles could also be improved by engineering the structure of hydrophobic block by introducing aromatic moieties.[24,25]

We have successfully synthesized PEG-PCD lipopolymer with two different approaches (Figure 1). However, the first approach was selected due to the relative simplicity in the synthesis process, which is critical for its application. In this synthesis approach, PEG-PBC was synthesized by ring-opening polymerization of MBC in the presence of PEG carrying a hydroxyl end group with one of the following catalysts: DBU, Sn(oct)$_2$, and Et$_2$Zn (Table 1). Relatively lower reaction efficiency was observed with Sn(oct)$_2$ and Et$_2$Zn; this is due to the high reaction temperature and long reaction time required for these two catalysts, which is usually associated with the potential polymer degradation due to transesterification or backbiting side reaction.[24,26] In addition, the use of these metallic catalysts is also associated with safety issues due to the presence of trace metal residue in the polymer. Therefore, DBU was used in the current study, which is purely organic and suitable for the synthesis of biomaterials. Besides, the reaction was carried out in solution and at room temperature, which is superior to bulk reaction that usually results in broad polydispersity due to the inefficient mixing of reactants. To optimize the reaction time, molecular weight of the polymer was monitored during the reaction. We found that the reaction was almost completed after 3 h and the DP of polymerization decreased after reaction for 24 h. This may be due to the occurring of transesterification of polymer, which becomes dominant when the monomer is consumed.[26] Therefore, the reaction time was set to 3 h to achieve optimal polymerization efficiency and polydispersity. Subsequently, the benzyl groups in the PEG-PBC were removed via hydrogenation to expose COOH function group. This reaction was also carried out under at the room temperature to avoid the potential degradation of polymer backbone, while still maintaining the high reaction efficiency to completely remove benzyl groups. The dodecanol was conjugated to the COOH groups in the polymer backbone through EDC/HOBT coupling chemistry with conjugation efficiency of around 95%. This is much higher than the previous report, where less than 70% of conjugation efficiency was achieved in conjugating fatty acids to poly(ethylene glycol)-*block*-poly(β-benzyl-L-aspartate) through a link molecule.[27] Because of the commercial availability of starting materials, simple synthesis procedure, and high reaction efficiency, this synthesis procedure will have a broad application in the drug delivery and bioengineering.

PEG-PCD lipopolymer synthesized in the current study has the polycarbonate backbone and dodecanol was conjugated to this backbone with an ester bond. Therefore, this is a biodegradable polymer, which is expected to degrade in vivo through hydrolysis of the ester linkages. The hydrolysis of polycarbonate backbone was facilitated at the presence of esterase such as lipase or cholesterol esterase.[28,29] In addition, the final degradation product was CO$_2$, dual alcohol, dodecanol, and PEG$_{5000}$, which have less effect on pH change in vivo compared to poly(D,L-lactide) and thus are less likely to cause inflammation.[30] These degradation products are nontoxic and could be eliminated from the body.

PEG-PCD lipopolymer has multiple dodecanol lipid chains attached to the polycarbonate backbone, which mimics the structure of interface cross-linked PEG-lipids (Figure 13) and could enhance the hydrophobic interaction among the hydrophobic cores. Because the cross-linking of micelles are known to improve stability, it is not surprising to observe significantly reduced CMC values for PEG-PCD lipopolymer compared to conventional PEG-lipid conjugates. Due to its low CMC value ($\sim$10^{-8} M), the concentration of PEG-PCD in the bloodstream is expected to be much higher than the CMC value of PEG-
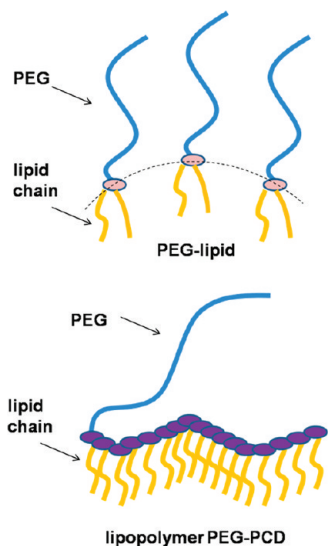
Figure 13. Structure of PEG-lipid and lipopolymer PEG-PCD.

Embelin

Figure 14. Structure of embelin and the repeating unit of the hydrophobic core.

PCD after systemic administration, which indicates its good in vivo stability. Therefore, PEG-PCD lipopolymer micelles can serve as an alternative to cross-linked PEG-lipid micelles for in vivo drug delivery.

Among PEG-PCD series, we found that the CMC decreased with increasing the number of lipid in the hydrophobic core (Figure 6B). This is due to the increased length of hydrophobic block, which is known to enhance the hydrophobic interaction among the core block.[31] The effects of core structure were also investigated and the results showed that the CMC of PEG-PCD or PEG-PBC was around 50-fold lower than corresponding PEG-PCC (Figure 6A). This is because of the presence of hydrophobic aromatic rings in PEG-PBC and lipid chains in PEG-PCD, which will all facilitate the hydrophobic interaction within the core of micelles and promote the self-assembly of polymeric micelles. However, PEG-PCC has a higher CMC due to the presence of COOH group which significantly reduced the hydrophobicity of the core block. Comparable CMC values were observed for PEG-PBC and PEG-PCD, though the structure of PBC and PCD are significantly different (Figure 6A). Because the backbone is the same for PEG-PBC and PEG-PCD, the close similarity in CMC values are due to comparable contributions by the pedant phenyl rings in the PBC and the pedant dodecanol carbon chain in PCD to the core block hydrophobicity.

Spherical, cylindrical, and vesicular assemblies are three commonly observed morphologies of micelles prepared from amphiphilic block copolymers. Recently, interest has shifted from spherical to cylindrical micelles due to their longer systemic circulation time compared to spherical micelles.[32–34] The cylindrical micelles prepared from poly(ethylene glycol)-*b*-poly(caprolactone) (PEG-PCL) showed significantly longer circulation time than that of spherical micelles prepared from the same polymer and was persistent up to several days after intravenous injection.[32] In addition, paclitaxel-loaded cylindrical micelles were more effective to induce apoptosis and reduce the tumor size in tumor bearing mice.[33,34] Several approaches have been investigated to control the morphology of micelles, including kinetic control,[35] the use of interfacial instability,[36] aromatic oxidation,[37] and the use of nanopore extruder.[38] The most important parameter that determines the morphology and architecture of micelles is the copolymer composition and volume ratio between insoluble and soluble blocks. Sumeet et
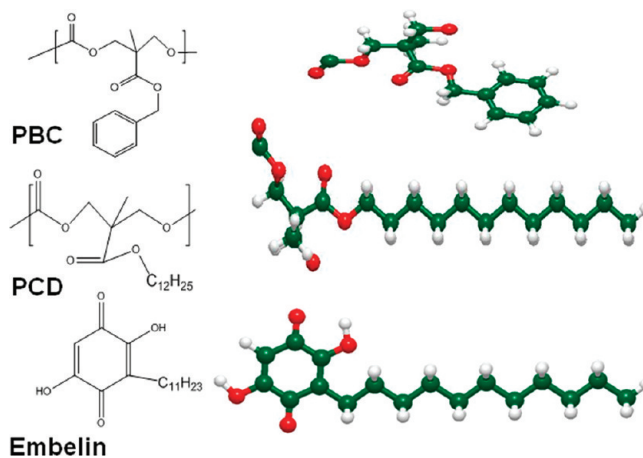
al. have studied the effect of molecular size and composition using poly(ethylene glycol)-*b*-poly(1,2-butadiene) (PEG-PB) as a model diblock copolymer. These authors found that PEG-PB form spheres, cylinders, and bilayers in water, sequentially, with decreased ratio of PEG block.[39] This could explain the transition from spherical to cylindrical micelles with the increased hydrophobic length of PEG-PCD. In the current study, the use of PEG-PCD$_{29}$ with a PEG ratio of 0.37 produced cylindrical micelles, while PEG-PCD$_6$ (PEG ratio: 0.49) and PEG-PCD$_{16}$ (PEG ratio: 0.72) produced only spherical micelles. Although PEG-PCD$_{29}$ formed cylindrical micelles, PEG-PBC$_{30}$, a polymer with similar hydrophobic core length did not form cylindrical micelles, but instead formed spherical micelles (Figure 10). This indicates that not only the PEG ratio but also the structure of hydrophobic core determines the morphology of micelles. Thus, the morphology of micelles can be controlled by changing the length and structure of the hydrophobic core of the polymer. The preparation of micelles of different morphologies will help us to understand the effect of micelles morphology and their in vivo biodistribution and bioactivities.

The compatibility of core-forming block and the drug to be loaded is critical for drug loading capacity.[12] One objective of this study was to design an engineered polymeric micelle for improved solubilization and delivery of embelin based on the polymer−drug compatibility. PEG-PCD showed significantly high embelin loading capacity compared with PEG-PBC (Figure 7), although these two polymers have similar CMC value and comparable thermodynamic stability. The compatibility is highly dependent on the three-dimensional arrangement and conformation of different groups in the structure of drug and polymer core.[25] Figure 14 illustrates the structure of embelin and the repeating units of the PEG-PBC and PEG-PCD hydrophobic core block. In contrast to PEG-PBC, the structure of the repeating unit of PEG-PCD is similar to that of embelin. A similar finding was reported previously, where the attachment of cholesterol to the poly(caprolactone) block of a poly(ethylene glycol)-*b*-poly(caprolactone) copolymer significantly improved the loading of cucurbitacin I, which is similar to cholesterol in the structure.[25] Our previous data also showed that the introduction of carbonate moiety into a PEG-PLA copolymer significantly increased the micellar solubility and loading of bicalutamide into micelles.[12] In this study, we also found that PEG-PCD lipopolymers with different core block lengths (repeating unit number ranges from 6 to 29) did not show significant differences in the drug loading (Figure 7). Although an increased drug loading efficiency was observed with an increased length

of PCL blocks in PEG-PCL polymer,[40] this may not be applicable for PEG-PCD, which has a highly branched structure in contrast to the linear structure of PEG-PCL. In fact, a good drug loading was observed in PEG-lipid conjugates with a much shorter hydrophobic core length,[3] indicating that the further increase in hydrophobic length might not be able to improve the drug loading of lipopolymers with similar structure as PEG-PCD. Similarly, we also observed there was no significant difference in the in vitro drug release profiles among these PEG-PCD polymers with different block lengths (Figure 11A). The drug release profiles of polymeric micelles are influenced by several factors including strength of the interaction between drug and hydrophobic core, physical state of the core, the amount of drug loaded, the length of the hydrophobic core, and the location of the drug inside the micelle core.[31] In addition, the highly branched structure in the hydrophobic core of PEG-PCD may have contributed to the observation in this study. We also found that the release of embelin from PEG-PCD was much slower than that from PEG-PBC (Figure 11B). This might due to the fact that the interaction between PEG-PCD and embelin was stronger than those of PEG-PBC and embelin.

5. Conclusion

We have successfully synthesized a novel lipopolymer poly(ethylene glycol)-*block*-poly(2-methyl-2-carboxyl-propylene carbonate-graft-dodecanol) (PEG-PCD) for delivery of a hydrophobic anticancer drug, embelin. PEG-PCD lipopolymer could form micelles in water through self-assembly and significantly improved embelin solubility by loading drugs inside its hydrophobic core. The drug loading and encapsulation efficiency were dependent on the length and structure of the polymer hydrophobic core block. The CMC of PEG-PCD micelles was around 10^{-8} M and decreased with increasing the length of hydrophobic block, indicating good thermodynamic stability of PEG-PCD micelles. The particle size and morphology of micelles were also dependent on the structure and length of the hydrophobic core. Embelin-loaded PEG-PCD micelles showed significant inhibition of C4-2 prostate cancer cell proliferation in a dose-dependent manner, while no obvious cellular toxicity was observed with blank micelles themselves. Thus, these lipopolymer have the potential to be used as vehicles for anticancer hydrophobic drug delivery.

Supporting Information Available. (1) ^{1}H NMR of 2-methyl-2-carboxyl-propylene carbonate (MCC) in DMSO and 2-methyl-2-dodecanoxycarbonyl-propylene carbonate (MDC) in CDCl$_3$. (2) Transmission electron microscopy (TEM) of embelin-loaded micelles (A) PEG$_{114}$-PCD$_6$, (B) PEG$_{114}$-PCD$_{16}$, (C) PEG$_{114}$-PCD$_{29}$, and (D) PEG$_{114}$-PBC$_{30}$. This material is available free of charge via the Internet at http://pubs.acs.org.

References and Notes

(1) Hennenfent, K. L.; Govindan, R. Novel formulations of taxanes: a review. Old wine in a new bottle. *Ann. Oncol.* **2006**, *17* (5), 735–49.

(2) Gaucher, G.; Marchessault, R. H.; Leroux, J. C. Polyester-based micelles and nanoparticles for the parenteral delivery of taxanes. *J. Controlled Release* **2010**, *143* (1), 2–12.

(3) Lukyanov, A. N.; Torchilin, V. P. Micelles from lipid derivatives of water-soluble polymers as delivery systems for poorly soluble drugs. *Adv. Drug Delivery Rev.* **2004**, *56* (9), 1273–89.

(4) Torchilin, V. P. Lipid-core micelles for targeted drug delivery. *Curr. Drug Delivery* **2005**, *2* (4), 319–27.

(5) Kabanov, A. V.; Batrakova, E. V.; Alakhov, V. Y. Pluronic block copolymers as novel polymer therapeutics for drug and gene delivery. *J. Controlled Release* **2002**, *82* (2–3), 189–212.

(6) Kabanov, A. V.; Batrakova, E. V.; Alakhov, V. Y. Pluronic block copolymers for overcoming drug resistance in cancer. *Adv. Drug Delivery Rev.* **2002**, *54* (5), 759–79.

(7) Kabanov, A. V.; Batrakova, E. V.; Alakhov, V. Y. An essential relationship between ATP depletion and chemosensitizing activity of Pluronic block copolymers. *J. Controlled Release* **2003**, *91* (1–2), 75–83.

(8) Jeong, B.; Bae, Y. H.; Lee, D. S.; Kim, S. W. Biodegradable block copolymers as injectable drug-delivery systems. *Nature* **1997**, *388* (6645), 860–2.

(9) Nishiyama, N.; Kataoka, K. Current state, achievements, and future prospects of polymeric micelles as nanocarriers for drug and gene delivery. *Pharmacol. Ther.* **2006**, *112* (3), 630–48.

(10) Danquah, M.; Li, F.; Duke, C. B., 3rd; Miller, D. D.; Mahato, R. I. Micellar delivery of bicalutamide and embelin for treating prostate cancer. *Pharm. Res.* **2009**, *26* (9), 2081–92.

(11) Yasugi, K.; Nagasaki, Y.; Kato, M.; Kataoka, K. Preparation and characterization of polymer micelles from poly(ethylene glycol)-poly(D,L-lactide) block copolymers as potential drug carrier. *J. Controlled Release* **1999**, *62* (1–2), 89–100.

(12) Danquah, M.; Fujiwara, T.; Mahato, R. I. Self-assembling methoxy-poly(ethylene glycol)-*b*-poly(carbonate-*co*-L-lactide) block copolymers for drug delivery. *Biomaterials* **2010**, *31* (8), 2358–70.

(13) Lavasanifar, A.; Samuel, J.; Kwon, G. S. Micelles of poly(ethylene oxide)-*block*-poly(*N*-alkyl stearate L-aspartamide): synthetic analogues of lipoproteins for drug delivery. *J. Biomed. Mater. Res.* **2000**, *52* (4), 831–5.

(14) Lavasanifar, A.; Samuel, J.; Kwon, G. S. Micelles self-assembled from poly(ethylene oxide)-*block*-poly(*N*-hexyl stearate L-aspartamide) by a solvent evaporation method: effect on the solubilization and haemolytic activity of amphotericin B. *J. Controlled Release* **2001**, *77* (1–2), 155–60.

(15) Li, F.; Lu, Y.; Li, W.; Miller, D. D.; Mahato, R. I. Synthesis, formulation and in vitro evaluation of a novel microtubule destabilizer, SMART-100. *J. Controlled Release* **2010**, *143* (1), 151–8.

(16) Koester, L. S.; Ortega, G. G.; Mayorga, P.; Bassani, V. L. Mathematical evaluation of in vitro release profiles of hydroxypropylmethylcellulose matrix tablets containing carbamazepine associated to beta-cyclodextrin. *Eur. J. Pharm. Biopharm.* **2004**, *58* (1), 177–9.

(17) Yamamoto, T.; Yokoyama, M.; Opanasopit, P.; Hayama, A.; Kawano, K.; Maitani, Y. What are determining factors for stable drug incorporation into polymeric micelle carriers? Consideration on physical and chemical characters of the micelle inner core. *J. Controlled Release* **2007**, *123* (1), 11–8.

(18) Leung, S. Y.; Jackson, J.; Miyake, H.; Burt, H.; Gleave, M. E. Polymeric micellar paclitaxel phosphorylates Bcl-2 and induces apoptotic regression of androgen-independent LNCaP prostate tumors. *Prostate* **2000**, *44* (2), 156–63.

(19) Maeda, H.; Wu, J.; Sawa, T.; Matsumura, Y.; Hori, K. Tumor vascular permeability and the EPR effect in macromolecular therapeutics: a review. *J. Controlled Release* **2000**, *65* (1–2), 271–84.

(20) Greish, K.; Nagamitsu, A.; Fang, J.; Maeda, H. Copoly(styrene-maleic acid)-pirarubicin micelles: high tumor-targeting efficiency with little toxicity. *Bioconjugate Chem.* **2005**, *16* (1), 230–6.

(21) Shuai, X.; Merdan, T.; Schaper, A. K.; Xi, F.; Kissel, T. Core-cross-linked polymeric micelles as paclitaxel carriers. *Bioconjugate Chem.* **2004**, *15* (3), 441–8.

(22) Xu, Y.; Meng, F.; Cheng, R.; Zhong, Z. Reduction-sensitive reversibly crosslinked biodegradable micelles for triggered release of doxorubicin. *Macromol. Biosci.* **2009**, *9* (12), 1254–61.

(23) Tian, L.; Yan, L.; Wang, J.; Tat, H.; Uhrich, K. Core crosslinkable polymeric micelles from PEG-lipid amphiphiles as drug carriers. *J. Mater. Chem.* **2004**, *14*, 2317–2324.

(24) Mahmud, A.; Xiong, X.; Lavasanifar, A. Novel self-associating poly(ethylene oxide)-*block*-poly(epsilon-caprolactone) block copolymers with functional side groups on the polyester block for drug delivery. *Macromolecules* **2006**, *39*, 9419–28.

(25) Mahmud, A.; Patel, S.; Molavi, O.; Choi, P.; Samuel, J.; Lavasanifar, A. Self-associating poly(ethylene oxide)-*b*-poly(α-cholesteryl carboxylate-ε-caprolactone) block copolymer for the solubilization of STAT-3 inhibitor Cucurbitacin I. *Biomacromolecules* **2009**, *10* (3), 471–478.

(26) Seow, W. Y.; Yang, Y. Y. Functional polycarbonates and their self-assemblies as promising nonviral vectors. *J. Controlled Release* **2009**, *139* (1), 40–7.

(27) Lavasanifar, A.; Samuel, J.; Kwon, G. S. The effect of fatty acid substitution on the in vitro release of amphotericin B from micelles composed of poly(ethylene oxide)-*block*-poly(*N*-hexyl stearate-L-aspartamide). *J. Controlled Release* **2002**, *79* (1−3), 165–72.

(28) Zhu, K.; Hendren, R.; Jensen, K.; Pitt, C. Synthesis, properties, and biodegradation of poly(1,3-trimethylene carbonate. *Macromolecules* **1991**, *24* (8), XXX.

(29) Tang, Y. W.; Labow, R. S.; Santerre, J. P. Enzyme-induced biodegradation of polycarbonate-polyurethanes: Dose dependence effect of cholesterol esterase. *Biomaterials* **2003**, *24* (12), 2003–11.

(30) Gao, J.; Guo, Y.; Gu, Z.; Zhang, X. Micellization and controlled release properties of methoxy poly(ethylene glycol)-*b*-poly(D,L-lactide-*co*-trimethylene carbonate. *Front. Chem. China* **2009**, *4* (1), .

(31) Allen, C.; Maysinger, D.; Eisenberg, A. Nano-engineering block copolymer aggregates for drug delivery. *Colloids Surf., B* **1999**, *16*, 3–27.

(32) Geng, Y.; Dalhaimer, P.; Cai, S.; Tsai, R.; Tewari, M.; Minko, T.; Discher, D. E. Shape effects of filaments versus spherical particles in flow and drug delivery. *Nat. Nanotechnol.* **2007**, *2* (4), 249–55.

(33) Cai, S.; Vijayan, K.; Cheng, D.; Lima, E. M.; Discher, D. E. Micelles of different morphologies—advantages of worm-like filomicelles of PEO-PCL in paclitaxel delivery. *Pharm. Res.* **2007**, *24* (11), 2099–109.

(34) Christian, D. A.; Cai, S.; Garbuzenko, O. B.; Harada, T.; Zajac, A. L.; Minko, T.; Discher, D. E. Flexible filaments for in vivo imaging and delivery: persistent circulation of filomicelles opens the dosage window for sustained tumor shrinkage. *Mol. Pharm.* **2009**, *6* (5), 1343–52.

(35) Cui, H.; Chen, Z.; Zhong, S.; Wooley, K. L.; Pochan, D. J. Block copolymer assembly via kinetic control. *Science* **2007**, *317* (5838), 647–50.

(36) Zhu, J.; Hayward, R. C. Spontaneous generation of amphiphilic block copolymer micelles with multiple morphologies through interfacial Instabilities. *J. Am. Chem. Soc.* **2008**, *130* (23), 7496–502.

(37) Baram, J.; Shirman, E.; Ben-Shitrit, N.; Ustinov, A.; Weissman, H.; Pinkas, I.; Wolf, S. G.; Rybtchinski, B. Control over self-assembly through reversible charging of the aromatic building blocks in photofunctional supramolecular fibers. *J. Am. Chem. Soc.* **2008**, *130* (45), 14966–7.

(38) Chen, Q.; Zhao, H.; Ming, T.; Wang, J.; Wu, C. Nanopore extrusion-induced transition from spherical to cylindrical block copolymer micelles. *J. Am. Chem. Soc.* **2009**, *131* (46), 16650–1.

(39) Jain, S.; Bates, F. S. On the origins of morphological complexity in block copolymer surfactants. *Science* **2003**, *300* (5618), 460–4.

(40) Park, E. K.; Lee, S. B.; Lee, Y. M. Preparation and characterization of methoxy poly(ethylene glycol)/poly(ε-caprolactone) amphiphilic block copolymeric nanospheres for tumor-specific folate-mediated targeting of anticancer drugs. *Biomaterials* **2005**, *26* (9), 1053–61.